

Low-temperature synthesis of high-purity single-walled carbon nanotubes from alcohol

Shigeo Maruyama^{a*}, Ryosuke Kojima^a, Yuhei Miyauchi^a, Shohei Chiashi^a, Masamichi Kohno^b

^a*Department of Mechanical Engineering, The University of Tokyo
7-3-1 Hongo, Bunkyo-ku, Tokyo 113-8656, Japan*

^b*National Institute of Advanced Industrial Science and Technology
Namiki 1-2-1, Tsukuba, Ibaragi 305-8564, Japan
Received 27 April 2002; in final form 7 May 2002*

Abstract

By using alcohol as the carbon source, a new simple catalytic chemical vapor deposition technique to synthesize high-purity single-walled carbon nanotubes at low temperature is demonstrated. Because of the etching effect of decomposed OH radical attacking carbon atoms with a dangling bond, impurities such as amorphous carbon, multi-walled carbon nanotubes, metal particles and carbon nanoparticles are completely suppressed even at relatively low reaction temperature such as 700 – 800 °C. By using methanol, generation of SWNTs even at 550 °C is demonstrated. The high-purity synthesis at low temperature promises large scale production at low cost and the direct growth of SWNTs on conventional semiconductor devices already patterned with aluminum.

1. Introduction

The discovery of single walled carbon nanotubes (SWNTs) [1] in 1993 has promised a new field of science and technology with their specially elongated fullerene structure. However, researchers could really join the game after the developments of high-quality macroscopic generation techniques of SWNTs by the pulsed laser-oven technique [2] and later by the electric arc-discharge technique [3]. In the last few years, the technique of catalytic chemical vapor deposition (CCVD) has been developed [4-21] for the expected larger-scale production [7-17] and for the controlled synthesis directly on semiconductor materials [18-21]. Following suggestions of the generation of SWNTs by the disproportional reaction of CO [4] or decomposition of benzene [11], various carbon-containing molecules such as CO [4,6,15,16], methane [5,7-10,14,18-21], ethylene [6,19], acetylene [12] and benzene [11] were tried in combinations with supported or floated fine metal catalysts. Recently, relatively pure SWNTs were generated by controlled preparations of metal fine particles of Fe, Ni, Co, Mo or mixtures supported by Al₂O₃, SiO₂ or MgO [7-9]. In addition, the continuous gas phase technique was also developed using floated catalyst particles coalesced from metallocene such as ferrocene [11,13] or iron pentacarbonyl (Fe(CO)₅) [12,15,16] supplied with carbon source gas to the high-temperature reaction zone. This technique could be scaled up as the well-developed VGCF (vapor-grown carbon fiber) technique [22]. Especially, the so-called HiPco process [15-17] using the disproportionation reaction of

* Corresponding Author. Fax: +81-3-5800-6983.

E-mail address: maruyama@photon.t.u-tokyo.ac.jp (S. Maruyama).

high-pressure and high-temperature CO with $\text{Fe}(\text{CO})_5$ as a catalyst seed is producing almost amorphous-free commercial SWNTs. Remaining problems of this technique are metal particles enclosed in carbon spherical shell [17] and the risk in the handling of CO. On the other hand, highly controlled generation of aligned SWNTs between electrodes on porous Si surface was also demonstrated [21]. The only impedance to the growth of SWNTs on semiconductor devices seems to be the high reaction temperature, 900 °C.

Here we report a simple, high-purity and low-temperature synthesis of SWNTs by using a new carbon source molecule, alcohol. Except for the carbon source, usual CCVD techniques using Fe/Co catalysts supported with zeolite [23, 24] were employed. The use of alcohol is rather controversial because much less formation of soot, or solid carbon, is known from an alcohol flame compared to a hydrocarbon flame [25]. It turned out that competing reactions of forming SWNTs and etching amorphous carbon on the catalyst surface was the key of high-purity and low-temperature synthesis of SWNTs. The lower reaction temperature and the high-purity features of this alcohol CCVD technique guarantee easy scale-up production at a lower cost. Furthermore, the reaction temperature lower than 600 °C ensures that this technique can be easily applicable for the direct growth of SWNTs on semiconductor devices already patterned with aluminum. Finally, because this technique is so simple and safe, pure SWNTs can be immediately synthesized at any physics, chemistry or engineering laboratories.

2. Experimental

The metal catalyst supported with zeolite was prepared according to the recipe of Shinohara's group [23, 24]. In brief, iron acetate $(\text{CH}_3\text{CO}_2)_2\text{Fe}$ and cobalt acetate $(\text{CH}_3\text{CO}_2)_2\text{Co}\cdot 4\text{H}_2\text{O}$ were dissolved in ethanol (typically 20 ml) and mixed with Y-type zeolite powder [HSZ-390HUA] (typically 1g). The amounts of Fe and Co were 2.5 wt % each. The solution was then sonicated for 10 minutes and dried for 24 hours at 80 °C. The resultant white-yellow powder on the quartz boat was placed in a quartz tube (i.d. 27 mm) inside of an electric furnace. While heating up to the desired reaction temperature, more than 200 sccm Ar flow was kept. When the boat reached the desired temperature in about 30 minutes, Ar gas was evacuated and alcohol vapor was supplied to the quartz tube for typically 10 minutes from a room temperature reservoir. Keeping the vacuum pump on, the pressure of ethanol in the quartz tube was typically about 5 Torr. By controlling the reservoir temperature, the vapor pressure was varied. After cooling down, the blackened sample on the boat was analyzed with Raman spectrometry, scanning electron microscopy (SEM) and transmission electron microscopy (TEM).

3. Results and discussion

Figure 1 shows a TEM image of 'as grown' SWNTs from ethanol at 800 °C. The sample was sonicated in ethanol and a drop was evaporated on the microgrid. As we carefully scanned the TEM for several hours, we could rarely observe amorphous carbon, multi-walled carbon nanotubes (MWNTs), carbon nanoparticles or metal particles. Only SWNTs and zeolite particles were observed. Isolated or small bundles of SWNTs with about 1 nm diameter with clean tube-walls are apparent in Fig. 1. SWNTs generated with laser-oven or arc-discharge techniques usually have clean tube-walls but SWNTs from CCVD usually suffers from imperfect tube-wall structures as a result of imperfect annealing of nanotubes. In addition, most of the samples are contaminated with various side products such as amorphous carbon. We believe that Fig. 1 is one of the cleanest images of 'as grown' SWNTs ever reported. With lower reaction temperature such as 600 °C for ethanol, some view in the TEM projection was occupied with SWNTs as in Fig. 1, but in certain spots there were insufficiently annealed short MWNTs with small metal particles at the end. It seems that the catalyst

condition or alcohol gas flow condition was not always perfect at low temperature. By optimizing these conditions, probably a better sample can be produced at even lower temperature.

Figure 2 shows a TEM image with lower magnification and a SEM image of the sample generated in the same condition as in Fig. 1. From this TEM image in panel A, it can be confirmed that the high-purity image in Fig. 1 is not a specially selected view of the sample. For the SEM image in panel B, a small amount of 'as grown' sample was placed with a conductive tape used for the observation. Web-like growth of bundles of SWNTs from zeolite particles around 300 nm is observed. Again, no other structures such as amorphous carbon are observed from both panels A and B.

Effects of reaction temperature, reaction pressure, kinds of alcohol and catalysts were studied mostly with the Raman measurement [26] by a homemade macro-Raman apparatus with a 50 cm single monochromator and a CCD detector. Figure 3 compares Raman spectra of 'as grown' sample from ethanol for various oven temperatures. The excitation wavelength was 488 nm with an Ar ion laser. The clear radial breathing modes (RBM) ($150\text{-}300\text{ cm}^{-1}$) and the G-band with the zone-holding spread (about 1590 cm^{-1}) for all spectra were observed. As a reference, the bottom spectrum was measured from a sample generated with the laser oven technique with Ni/Co (0.6 wt% each) loaded graphite. The D-band signal (about 1350 cm^{-1}) was quite small for the $700\text{ - }900\text{ }^{\circ}\text{C}$ cases but was considerably larger for the $600\text{ }^{\circ}\text{C}$ case. The D-band increase for $600\text{ }^{\circ}\text{C}$ was probably because of the short MWNTs observed in the TEM image. From the expanded RBM signal in panel A, the diameter of SWNTs was estimated to be typically $0.8\text{ - }1.2\text{ nm}$. Here, the following correlation [27, 28] between diameter d (nm) and RBM Raman shift λ (cm^{-1}): $d = 248/\lambda$ was used for the upper coordinate in panel A. In comparison with the Ni/Co loaded graphite in the laser-oven technique (panel A(e)), the tube diameter is smaller and more widely distributed. With decreasing reaction temperature, the diameter distribution shifted to the thinner side. At the same time, the BWF line shape [26, 29], which is characteristic of metal SWNTs, is clearly seen for lower temperature samples. From a detailed comparison with the Kataura plot [29], the Raman peaks around $150\text{-}220\text{ cm}^{-1}$ are assigned to semiconductor SWNTs and the peaks in $230\text{-}300\text{ cm}^{-1}$ to metallic SWNTs. The temperature dependence of diameter distribution is very similar to the laser-oven technique [30, 31] even though the absolute value of temperature was much lower in our case.

By replacing ethanol to methanol, an almost identical Raman spectrum was observed at $800\text{ }^{\circ}\text{C}$ reaction as shown in Fig. 4, but nanotubes with slightly larger diameters were enhanced with the methanol case than with the ethanol case. Very similar Raman spectra were observed for the lowest temperature case, at $550\text{ }^{\circ}\text{C}$ with methanol and the $600\text{ }^{\circ}\text{C}$ case with ethanol, both from the D-band strength in panel B and the diameter distribution in panel A. Though the D-band peak was appreciable, it was clear that a substantial amount of SWNTs was generated at this low temperature. A comparison of the Raman spectra for ethanol and methanol indicated that the optimum reaction temperature was about $50\text{ }^{\circ}\text{C}$ lower for the methanol case. By TEM observations of the sample from methanol, we found that the bundle size was significantly smaller than the ethanol case, and there were small amounts of fine metal particles dispersed in bundles of SWNTs. We also quickly tried 1-propanol as another alcohol carbon source. Very similar results to those with ethanol were observed from the Raman measurements.

The reason why alcohols were much better carbon sources for SWNTs than hydrocarbons is explained by the role of decomposed OH radicals as follows. It is known that an OH radical efficiently removes the amorphous carbon in the purification process of SWNTs using H_2O_2 [32]. It is also known that the reaction of OH radical to solid carbon reduces the formation of soot in combustion chemistry [25]. Since an OH radical is decomposed on the catalyst surface from an alcohol molecule, it will attack nearby carbon atoms with a dangling bond to form CO. Then, seeds of amorphous carbon are efficiently removed in its very early stage. We believe that the initial stage

of MWNT formation in the CCVD process is also initiated from the amorphous carbon attaching to the SWNTs. Hence, the OH radical prohibits the generation of all these side-products, and only the SWNT can survive in this condition.

Different catalysts and supports were also quickly examined. Ni/Co metal mixtures instead of Fe/Co over zeolite gave a nearly identical result. Fe/Co supported with MgO prepared in the same procedure as the zeolite case was also successful. In the latter case, 3 % mixture of H₂ with Ar was used during a heating up process of the electric furnace. The lower pressure ethanol was preferred for this catalyst; however, the production of relatively high-purity SWNTs with ethanol at 800 °C was confirmed without further optimizations. This technique to synthesize SWNTs using alcohols is believed to be quite versatile about the selection of metal catalysts.

Probably, alcohol is the best carbon source for low-temperature growth of SWNTs on semiconductor materials with various catalyst forms. Furthermore, lower reaction temperature would considerably contribute to the lower cost design of a scaled-up gas phase continuous reactor using floated catalysts from ferrocene or iron pentacarbonyl (Fe(CO)₅), though further studies are necessary for the increase in the yield of SWNTs.

Acknowledgements

The authors would like to thank Professor H. Shinohara (Nagoya University) for valuable discussions about the zeolite support, Professor A. Tezaki (The University of Tokyo) for useful discussions, and H. Tsunakawa (The University of Tokyo) for assistance in TEM measurements.

References

- [1] S. Iijima, T. Ichihara, *Nature* 363 (1993) 603.
- [2] A. Thess, R. Lee, P. Nikolaev, H. Dai, P. Petit, J. Robert, C. Xu, Y. H. Lee, S. G. Kim, A. G. Rinzler, D. T. Colbert, G. E. Scuseria, D. Tománek, J. E. Fischer, R. E. Smalley, *Science* 273 (1996) 483.
- [3] C. Journet, W. K. Maser, P. Bernier, A. Loiseau, M. L. de la Chapelle, S. Lefrant, P. Deniard, R. Lee, J. E. Fisher, *Nature* 388 (1997) 756.
- [4] H. Dai, A. G. Rinzler, P. Nikolaev, A. Thess, D. T. Colbert, R. E. Smalley, *Chem. Phys. Lett.* 260 (1996) 471.
- [5] J. Kong, A. M. Cassell, H. Dai, *Chem. Phys. Lett.*, 292 (1998) 567.
- [6] J. H. Hafner, M. J. Bronikowski, B. R. Azamian, P. Nikolaev, A. G. Rinzler, D. T. Colbert, K. A. Smith, R. E. Smalley, *Chem. Phys. Lett.* 296 (1998) 195.
- [7] J.-F. Colomer, C. Stephan, S. Lefrant, G. V. Tendeloo, I. Willems, Z. Konya, A. Fonseca, Ch. Laurent, J. B. Nagy, *Chem. Phys. Lett.* 317 (2000) 83.
- [8] J.-F. Colomer, J.-M. Benoit, C. Stephan, S. Lefrant, G. Van Tendeloo, J. B. Nagy, *Chem. Phys. Lett.* 345 (2001) 11.
- [9] S. Tang, Z. Zhong, Z. Xiong, L. Sun, L. Liu, J. Lin, Z. X. Shen, K. L. Tan, *Chem. Phys. Lett.* 350 (2001) 19.
- [10] E. Flahaut, A. Govindaraj, A. Peigney, Ch. Laurent, A. Rousset, C.N.R. Rao, *Chem. Phys. Lett.* 300 (1999) 236.
- [11] H.M. Cheng, F. Li, X. Sun, S.D.M. Brown, M.A. Pimenta, A. Marucci, G. Dresselhaus, M.S. Dresselhaus, *Chem. Phys. Lett.* 289 (1998) 602.
- [12] B. C. Satishkumar, A. Govindaraj, R. Sen, C. N. R. Rao, *Chem. Phys. Lett.* 293 (1998) 47.
- [13] L. Ci, S. Xie, D. Tang, X. Yan, Y. Li, Z. Liu, X. Zou, W. Zhou, G. Wang, *Chem. Phys. Lett.* 349 (2001) 191.
- [14] M. Su, B. Zheng, J. Liu, *Chem. Phys. Lett.* 322 (2000) 321.

- [15] P. Nikolaev, M. J. Bronikowski, R. K. Bradley, F. Rohmund, D. T. Colbert, K. A. Smith, R. E. Smalley, *Chem. Phys. Lett.* 313 (1999) 91.
- [16] M. J. Bronikowski, P. A. Willis, D. T. Colbert, K. A. Smith, R. E. Smalley, *J. Vac. Sci. Technol. A* 19 (2001) 1800.
- [17] W. Zhou, Y. H. Ooi, R. Russo, P. Papanek, D. E. Luzzi, J. E. Fisher, M. J. Bronikowski, P. A. Willis, R. E. Smalley, *Chem. Phys. Lett.* 350 (2001) 6.
- [18] J. Kong, A. M. Cassell, H. Dai, *Nature* 395 (1998) 878.
- [19] J. H. Hafner, C.-L. Cheung, T. H. Oosterkamp, C. M. Lieber, *J. Phys. Chem. B* 105 (2001) 743.
- [20] Y. Li, W. Kim, Y. Zhang, M. Rolandi, D. Wang, H. Dai, *J. Phys. Chem. B* 105 (2001) 11424.
- [21] Y. Zhang, A. Chang, J. Cao, Q. Wang, W. Kim, Y. Li, N. Morris, E. Yenilmez, J. Kong, H. Dai, *Appl. Phys. Lett.* 79 (2001) 3155.
- [22] M. Endo, K. Takeuchi, K. Kobori, K. Takahashi, H. W. Kroto, A. Sarkar, *Carbon* 33 (1995) 873.
- [23] K. Mukhopadhyay, A. Koshio, N. Tanaka, H. Shinohara, *Jpn. J. Appl. Phys.* 37 (1998) L1257.
- [24] K. Mukhopadhyay, A. Koshio, T. Sugai, N. Tanaka, H. Shinohara, Z. Konya, J. B. Nagy, *Chem. Phys. Lett.* 303 (1999) 117.
- [25] J. Warnatz, U. Maas, R. W. Dibble, *Combustion: Physical and Chemical Fundamentals, Modeling and Simulation, Experiments, Pollutant Formation*, Springer-Verlag, Berlin, ed 3, 2001, p. 257.
- [26] A. M. Rao, E. Richter, S. Bandow, B. Chase, P. C. Eklund, K. A. Williams, S. Fang, K. R. Subbaswamy, M. Menon, A. Thess, R. E. Smalley, G. Dresselhaus, M. S. Dresselhaus, *Science* 275 (1997) 187.
- [27] R. Saito, G. Dresselhaus, M. S. Dresselhaus, *Phys. Rev. B* 61 (2000) 2981.
- [28] A. Jorio, R. Saito, J. H. Hafner, C. M. Lieber, M. Hunter, T. McClure, G. Dresselhaus, M. S. Dresselhaus, *Phys. Rev. Lett.* 86 (2001) 1118.
- [29] H. Kataura, Y. Kumazawa, Y. Maniwa, I. Umez, S. Suzuki, Y. Ohtsuka, Y. Achiba, *Synth. Met.* 103 (1999) 2555.
- [30] S. Bandow, S. Asaka, Y. Saito, A. M. Rao, L. Grigorian, E. Richter, P. C. Eklund, *Phys. Rev. Lett.* 80 (1998) 3779.
- [31] H. Kataura, Y. Kumazawa, Y. Maniwa, Y. Ohtsuka, R. Sen, S. Suzuki, Y. Achiba, *Carbon* 38 (2000) 1691.
- [32] H. Kataura, Y. Maniwa, T. Kodama, K. Kikuchi, K. Hirahara, K. Suenaga, S. Iijima, S. Suzuki, Y. Achiba, W. Krätschmer, *Synth. Met.* 121 (2001) 1195.

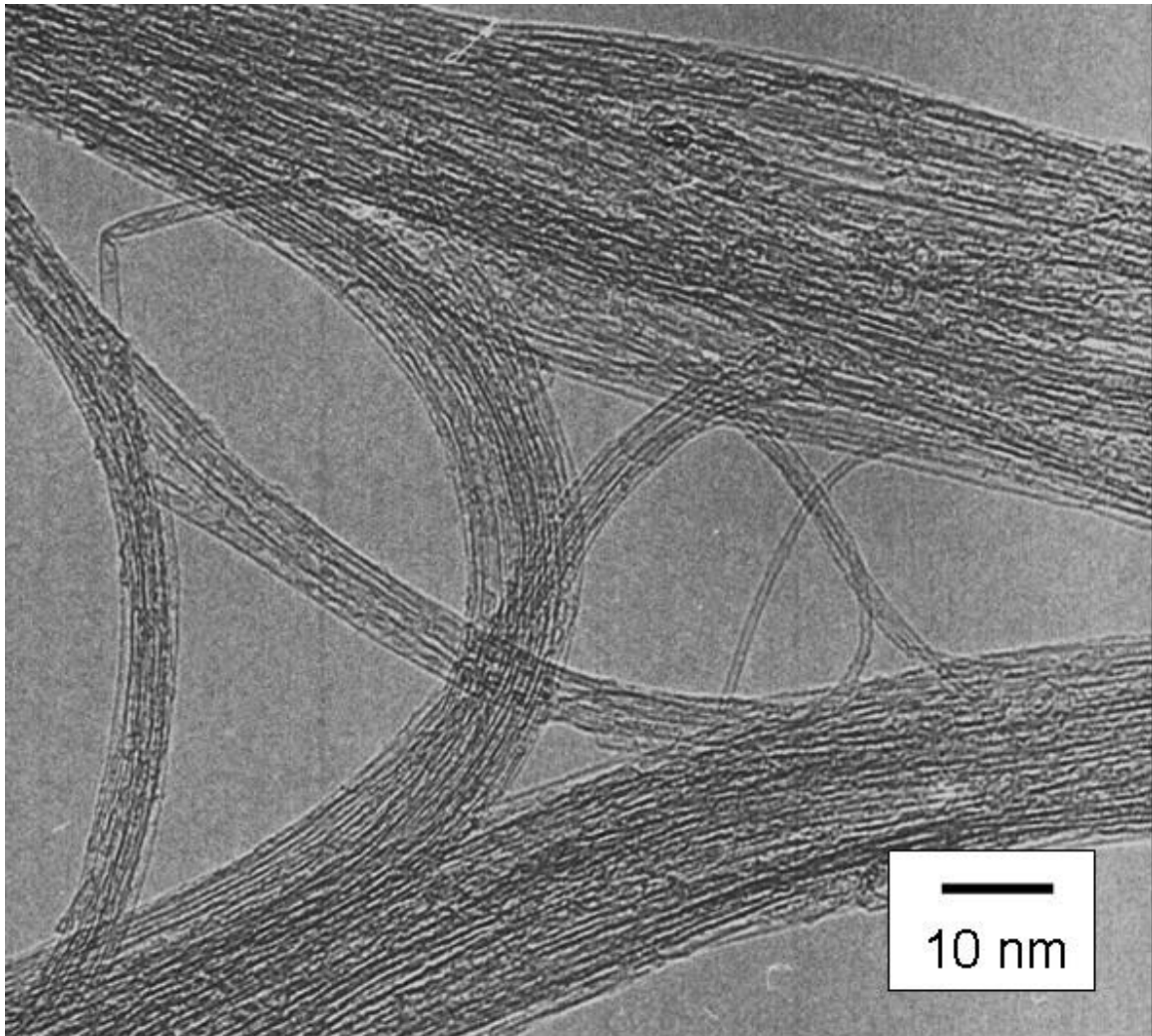


Fig. 1. TEM (200 kV) image of 'as grown' SWNTs by catalytic decomposition of ethanol over a Fe/Co mixture embedded in zeolite at 800 °C. There were isolated and bundles of SWNTs without MWNTs, amorphous carbon, carbon nanoparticles or metal particles.

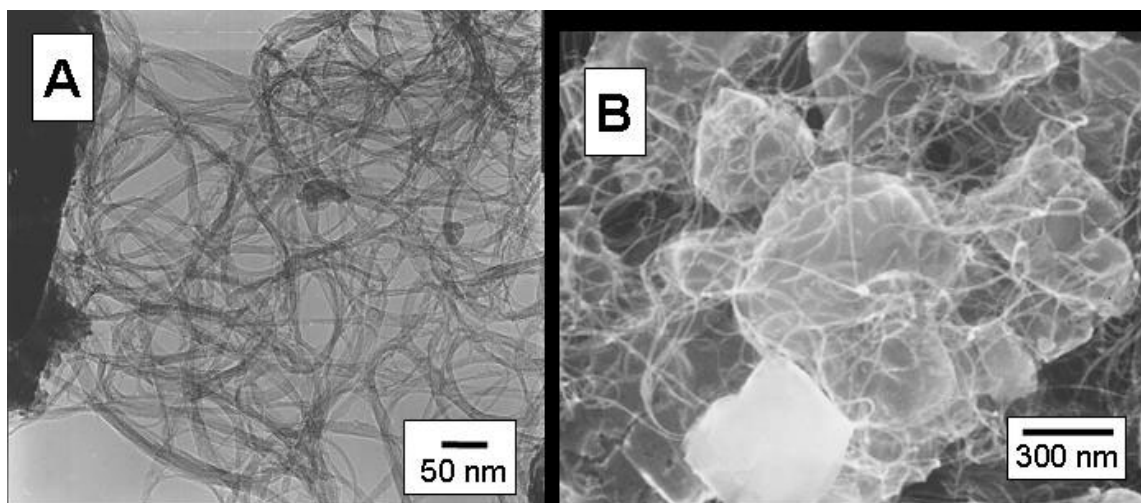


Fig. 2. Lower magnification TEM image (panel A) and SEM image (panel B) of 'as-grown' SWNTs by the same condition as in Fig. 1. Dark parts in the left of panel A is zeolite surface. Both in panels A and B, web-like growth of bundles of SWNTs covering zeolite particles around 300 nm were observed, nothing else.

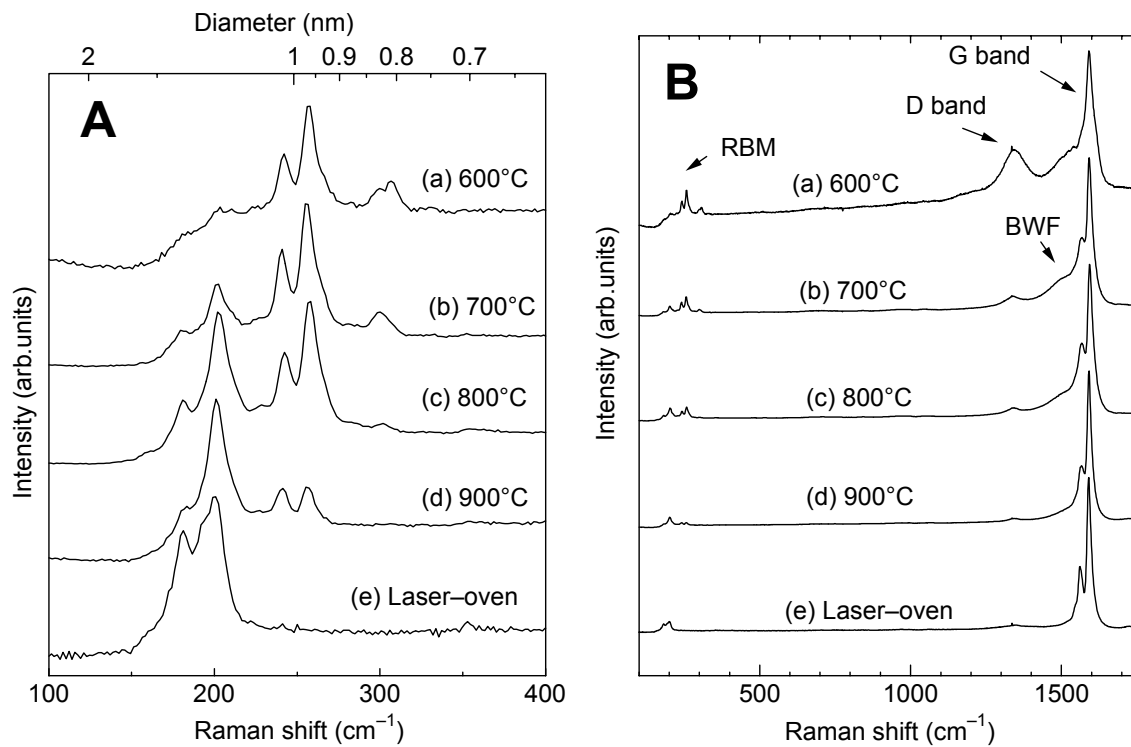


Fig. 3. Raman spectra of 'as-grown' SWNTs from ethanol over Fe/Co supported with zeolite at various temperatures (excitation at 488 nm). Panel A is an expanded view of low-frequency range of panel B. (a)-(d): CCVD from ethanol. (e): Laser-oven technique with Ni/Co-doped graphite at 1130 °C.

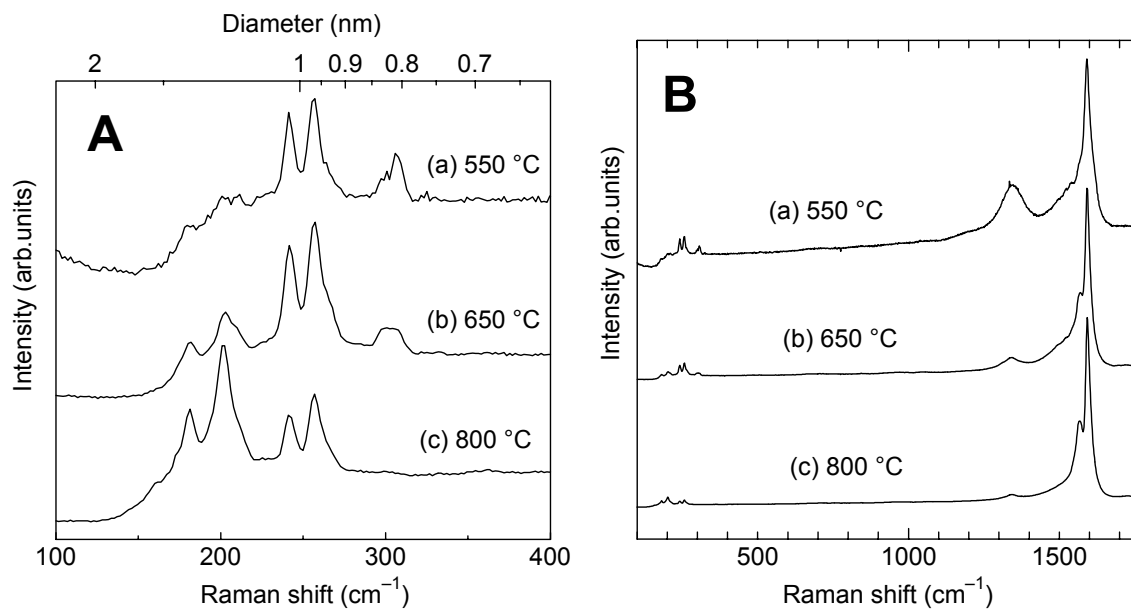


Fig. 4. Raman spectra of 'as-grown' SWNTs from methanol at relatively low temperatures. Panel A is an expanded view of low-frequency range. Note the shape of the Raman spectrum for methanol is similar to that at 50 °C higher temperature for ethanol in Fig. 3.